

Structure of Small Virus-like Particles Assembled from the L1 Protein of Human Papillomavirus 16

Xiaojiang S. Chen,^{*||} Robert L. Garcea,[‡]
Ilya Goldberg,^{*†} Gregory Casini,[‡]
and Stephen C. Harrison^{*†§}

^{*}Department of Molecular and Cellular Biology

[†]Howard Hughes Medical Institute

Harvard University

Cambridge, Massachusetts 02138

[‡]Section of Pediatric Hematology/Oncology

University of Colorado School of Medicine

Denver, Colorado 80262

Summary

The papillomavirus major late protein, L1, forms the pentameric assembly unit of the viral shell. Recombinant HPV16 L1 pentamers assemble *in vitro* into capsid-like structures, and truncation of ten N-terminal residues leads to a homogeneous preparation of 12-pentamer, icosahedral particles. X-ray crystallographic analysis of these particles at 3.5 Å resolution shows that L1 closely resembles VP1 from polyomaviruses. Surface loops contain the sites of sequence variation among HPV types and the locations of dominant neutralizing epitopes. The ease with which small virus-like particles may be obtained from L1 expressed in *E. coli* makes them attractive candidate components of a papillomavirus vaccine. Their crystal structure also provides a starting point for future vaccine design.

Introduction

Human papillomaviruses (HPVs) are pathogens of epithelial surfaces associated with both benign warts and malignant tumors (Howley, 1996; Shah and Howley, 1996). Over 90 HPV subtypes have been identified based on DNA sequence relationships. Strong epidemiologic and biochemical evidence supports association of infection by certain high-risk HPV subtypes (e.g., HPV16, 18, and 31) with subsequent development of human cervical cancer (Pisani et al., 1993; Bosch et al., 1995).

Papilloma virions contain two virally encoded proteins, L1 and L2, synthesized late in the infectious cycle. These two proteins encapsidate a histone-associated, closed circular, double-stranded DNA minichromosome. The outer shell of the virion contains 72 pentamers of L1, centered on the vertices of a $T = 7$ icosahedral lattice (Baker et al., 1991; Trus et al., 1997). L2, a largely internal protein, is present at about 1/30 the abundance of L1 (Kirnbauer et al., 1993). The overall surface organization of the papillomavirus shell resembles that of its close relatives, murine polyomavirus and SV40, which also contain 72 pentamers of a principal capsid protein,

VP1 (Rayment et al., 1982). Papillomavirus particles are somewhat larger than polyoma virions (600 Å diameter, rather than 500 Å), and they contain a correspondingly larger genome (8 kb rather than 5 kb) (Howley, 1996). Despite the close structural relationship, however, the genomic organization is distinct, and there is no discernible sequence similarity between L1 (about 500 residues) and VP1 (about 370 residues) (Belnap et al., 1996).

Recombinant expression of L1 using vaccinia, baculovirus, or yeast systems results in the formation of virus-like particles (VLPs), which are assemblies of roughly 72 L1 pentamers in a shell similar to that of the virion (Zhou et al., 1991a; Kirnbauer et al., 1992; Hagensee et al., 1993; Rose et al., 1993; Sasagawa et al., 1995). VLPs can induce neutralizing antibodies in inoculated animals, and immunization with VLPs can protect experimental animals from subsequent challenge with infectious virus (Breitburd et al., 1995; Suzich et al., 1995; Christensen et al., 1996). Thus, VLPs appear to be excellent candidates for papillomavirus vaccines.

Structural analysis of papillomavirus particles has been limited by an inability to grow large amounts of virus in culture and by a lack of success in obtaining suitable crystals of virions purified from warts. We have expressed the HPV16 L1 protein in *E. coli* and determined its crystal structure at 3.5 Å resolution. The crystallization conditions favor formation of a 12-pentamer, $T = 1$ icosahedral assembly of L1, which we describe as a "small VLP." Assembly experiments *in vitro* show that a short, N-terminal segment of the L1 polypeptide chain acts as a switch between 72-pentamer, virion-like assemblies and small VLPs. The L1 subunits have similar folded structures as their polyoma VP1 counterparts, but the modes of interpentamer association in polyoma virions and papilloma small VLPs are quite distinct. The L1 structure can be used to direct engineering of chimeric VLP vaccines (Greenstone et al., 1998), locate dominant neutralizing epitopes, identify mechanisms of neutralization by antibodies, and rationalize differences among viral serotypes.

Results and Discussion

Expression, Crystallization, and Assembly

We expressed HPV16 L1 and various truncated forms in *E. coli*, as glutathione S-transferase (GST) fusion proteins. Contrary to our expectations based on polyoma and SV40 VP1 (Liddington et al., 1991), deletions of up to 30 C-terminal residues had little or no effect on the stability or solubility of the expressed protein, or on the capacity of the appropriate N-terminally truncated protein to crystallize; C-terminal deletions longer than 30 residues rendered the L1 extremely sensitive to protease. N-terminal truncation was tolerated up to at least residue 13, but only products of constructs lacking 10 N-terminal residues (L1 Δ N-10) gave crystals suitable for structure determination. L1's with N-terminal deletions of 15 or more residues were unstable in the fusion

[§]To whom correspondence should be addressed (e-mail: schadmin@crystal.harvard.edu).

^{||}Present address: Department of Biochemistry and Molecular Genetics, University of Colorado School of Medicine, Denver, Colorado 80262.

Table 1. HPV16 L1 Truncations and Their Assembly Properties

Deletion	Trypsin Sensitivity	Apparent Diameter of Assembled Particle (Å) ^a
ΔN=0	No	600
ΔN=8	No	600
ΔN=9	No	600
ΔN=10	No	300
ΔN=15	Yes ^b	NA
ΔN=20	Yes	NA
ΔC=16	No	600
ΔC=30	No	600
ΔC=46	Yes	NA
ΔC=86	Yes	NA

ΔN/C-x: Δ designates deletion, N or C designates N or C terminus, and x designates number of deleted residues. All the N-terminal deletions were confirmed by seven cycles of N-terminal sequencing using Edman degradation. All the C-terminal deletions were confirmed by DNA sequencing. Trypsin sensitivity was used a measure of correct folding. The protease treatment was carried out while the GST-fused protein was still bound to glutathione beads (see Experimental Procedures). Sensitivity was determined by SDS-PAGE analysis of the beads after digestion.

^a Many of the 600 Å particles are imperfect, and there are particles of other sizes seen on the grid (Figure 1, left). The major species, however, is a shell with the approximate size of an HPV virion.

^b Most of the protein with this deletion is sensitive to digestion by trypsin, but about 5% resists degradation. NA, not applicable.

constructs we used (Table 1), and a form with 13 residues removed could not be cleaved from the GST.

We obtained several crystal forms of L1 ΔN-10, all with unit cells much larger than expected for isolated pentamers. The various buffers that yielded crystals had in all cases pH less than 6.4, and subsequent studies showed that low pH favors assembly of L1 into VLPs (Figure 1). The size and homogeneity of the observed particles depend on N-terminal truncation. L1 pentamers with up to nine N-terminal residues removed yield VLPs that resemble 72-pentamer virions (Figure 1, left). L1 pentamers with 10 residues removed yield 12-pentamer, small VLPs (Figure 1, center), and addition of

even a single glycine to the N terminus of the form lacking 10 residues switches assembly back to larger shells (Table 1). We were unable to test the effect of longer deletions on assembly, for reasons of expression yields outlined above and in Table 1. The first ordered residue in our structure of a small VLP is Lys-20, and we believe that had we been able to prepare suitable pentamers with up to about 19 N-terminal residues removed, we would probably have obtained T = 1 assemblies at low pH.

The presence of the N-terminal segment of L1 thus determines the size of the assembled particles. The structure described below shows that the N terminus of L1 indeed lies at interpentamer contacts. The assembly properties of L1 also determine successful crystallization. All crystals that we obtained were of the 12-pentamer particle. The 72-pentamer shells, formed by in vitro assembly of full-length L1, are too irregular for successful crystallization (see Figure 1).

Structure Determination

The structure was determined using a bloblike model to generate very low-resolution, "molecular replacement" phases, which were extended from 31 Å to about 17 Å by 20-fold noncrystallographic symmetry averaging. These phases were then used to locate mercury atoms in a derivative, and mercury single isomorphous replacement and noncrystallographic symmetry refinement were used together to complete the phasing at 3.5 Å. Additional details are given in the Experimental Procedures.

Description of the Structure

The T = 1 icosahedral assembly with 12 pentamers (Figure 2) has an outer diameter of 318 Å. Within each pentamer, the principal domains of the five L1 subunits associate intimately with each other, making a tightly linked ring. The less extensive, interpentameric contacts are formed by small, laterally projecting, elbow-like domains, which cluster around three-fold symmetry axes

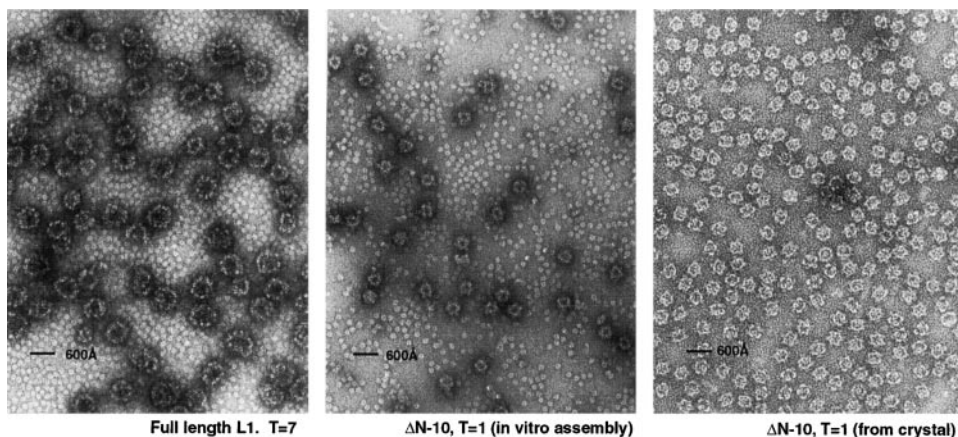


Figure 1. Assembly of Virus-like Particles from HPV16 L1 Pentamers, Monitored by Negative Stain Electron Microscopy

(Left) Particles that resemble 72-pentamer virions assemble at pH 5.2 from full-length L1. Note free pentamers in the background. (Center) Small, 12-pentamer VLPs assemble at pH 5.2 from L1 ΔN-10. Again, note free pentamers. (Right) Small VLPs derived from crystals, dissolved in low pH buffer. The staining is somewhat different than in the center panel because of the presence of some PEG, but close inspection shows the particles to be of indistinguishable morphology. Bars indicate 600 Å in all three panels.

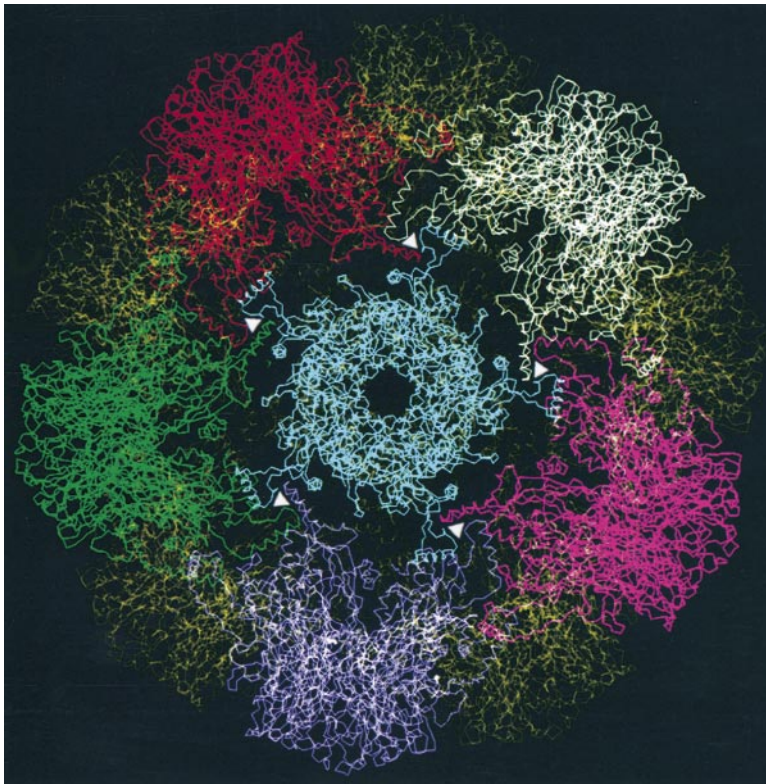


Figure 2. The $T = 1$ Particle of HPV16 L1
The view is near a five-fold axis. Each of the 12 identical L1 pentamers in this assembly is shown in a different color. The three-fold axes are shown by triangles. There are two-fold axes between each pair of three-fold axes.

(Figure 2). The complete particle thus has a markedly grooved appearance, with pentagonal "towers," decorated with stellate overhangs, rising above a more continuous "floor." The shape of these morphological units clearly corresponds to the pentamers seen by electron cryomicroscopy (Belnap et al., 1996; Trus et al., 1997).

The L1 Monomer

A classical "jelly roll" β sandwich, similar to the one found in polyoma and SV40 (Liddington et al., 1991), contains residues 20–382 of the 504-residue L1 polypeptide chain (Figures 3 and 4). The orientation of the long axis of the domain is approximately radial. Elaborate interstrand loops at one end impart a highly sculpted appearance to the outward-facing surface of the pentamer. The C-terminal lateral projections (residues 383–475, shown in yellow in Figure 3) are significantly α helical. Three helices (h2–4) form the surface of contact with other monomers, while a short strand (β J) and a final helix (h5) anchor the projection back to the jelly roll. The strand adds to the C edge of the CHEF sheet, and the helix tucks into the axial cavity of the pentamer, where it has a hydrophobic interface with the base of the BIDG sheet. The last 31 residues are disordered and project toward the interior of the particle. This segment, the most variable among L1 proteins of different papillomaviruses, is rich in basic residues as well as serine and threonine; it probably interacts with DNA in the virion, and it includes the L1 nuclear localization signal (Zhou et al., 1991b). In most of our preparations, some of the disordered, C-terminal tails have been cleaved, suggesting that they are very susceptible to proteolysis before assembly. Recombinant L1, fused at its C terminus to another small protein and expressed in insect

cells, can assemble into VLPs (Muller et al., 1997); it is likely that the fused element packs loosely into the interior of the VLP shell.

The Pentamer

The tightest contacts within a pentamer are at higher radii; the monomers splay apart toward the particle interior. The subunit orientation creates, along the pentamer axis, an inward-facing, conical hollow, which opens to the exterior of the particle through a narrow throat, about 14 Å in diameter. The polypeptide chain backbones of adjacent subunits interact directly. The G strand, at the inner margin of the BIDG sheet, "visits" the clockwise neighboring monomer and augments its CHEF sheet (see Figures 3A and 3C), before returning to rejoin its own subunit. The loops are also elaborately intertwined. The HI loop of one monomer, extending outward, inserts between the FG and EF loops of the anticlockwise neighbor and reaches far enough to contact the FG loop of the next neighbor; thus, there are, around the "top" of the pentamer, five overlapping bridges of paired HI:FG loops across an intervening subunit. Part of the EF loop extends outward to the edge of the pentamer, creating the five points of the starlike cap.

Pentamer–Pentamer Contacts

The only contacts between pentamers come from the small, laterally projecting domains (Figures 3A, 3C, and 3D). The first two helices (h2, h3) in the projecting domain form a V-shaped groove, into which fits the amino-terminal half of the longer, third helix (h4) from a three-fold related subunit. The contact is strongly hydrophobic (Figure 5). The third helix (h4) connects to and from the rest of the domain through an extended polypeptide chain, as if to create an adjustably oriented interaction

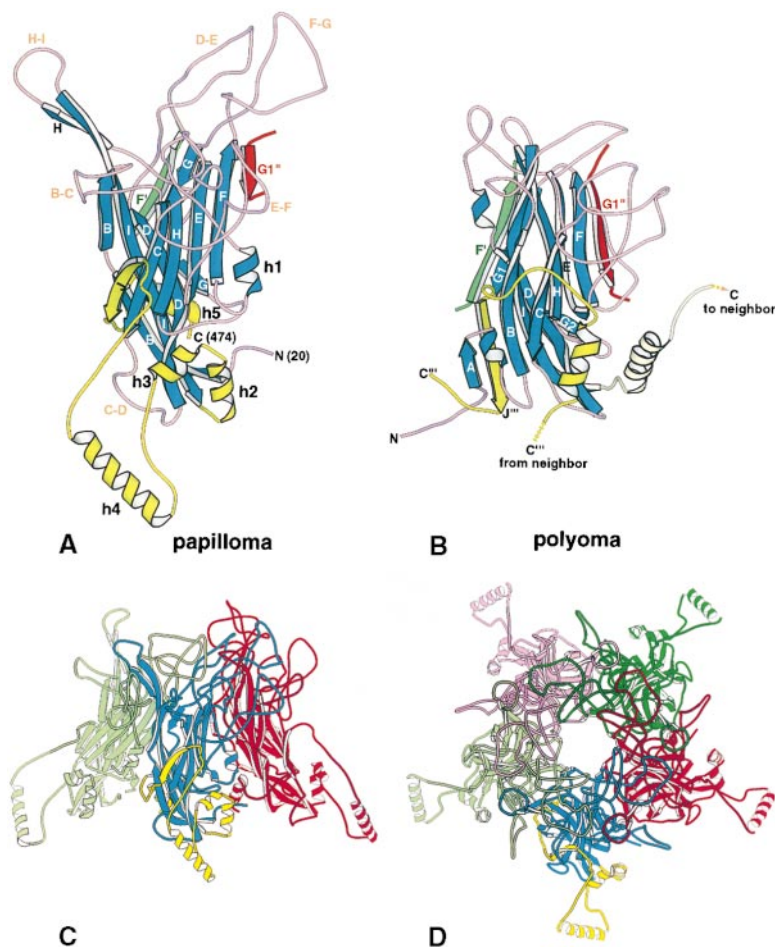


Figure 3. HPV16 L1 Monomer and Pentamer, with Polyomavirus VP1 Monomer for Comparison

(A) L1 monomer, viewed roughly normal to the five-fold axis of a pentamer. The structure includes residues 20–474; the first and last residues are labeled N(20) and C(474), respectively. The strands of the β jelly roll (and the short helix, h1, in the EF loop) are blue; connecting loops are pink; the G1 strand segment from the anticlockwise neighbor within a pentamer is red (this segment augments the CHEF sheet of the subunit, on the edge nearest the five-fold); the F strand of the clockwise neighbor is green (this is the edge of the sheet in the neighboring subunit with which the G1 segment forms hydrogen bonds); and the laterally projecting C-terminal domain is yellow. Strands (capital letters) and helices (h1–h5) are labeled, and the corresponding sequences can be identified from Figure 3. A primed label (F') denotes a segment of polypeptide chain from the clockwise neighbor within the pentamer; a double-primed label (G1''), one from the anticlockwise neighbor.

(B) Polyomavirus VP1 monomer, viewed in essentially the same direction as the L1 monomer in (A). Blue, pink, red, and green have the same significance as in the representation of L1; a C-terminal arm, “invading” from another pentamer (triple-primed letters), is yellow; the proximal part of the arm of the monomer in the figure, which extends into the neighboring pentamer, is light yellow; distal parts of this arm are not shown.

(C) L1 pentamer, viewed normal to the five-fold axis. The two monomers in the rear have been deleted for clarity. The C-terminal projection of the central (blue) monomer is shown in yellow.

(D) L1 pentamer, viewed along the five-fold axis from outside the particle. As in (C), the C-terminal projection of the blue monomer is yellow.

element. In the virion, with 72 rather than 12 pentamers, the details of this contact must vary. The linkage of h4 is likely to be a locus of such flexibility.

The interpentamer contacts are modest, leaving significant gaps in the vicinity of the two-fold axes (Figure 2). In virions, and in 72-pentamer VLPs, the corresponding gaps may be filled by parts of the amino-terminal segments, which are partly missing and partly disordered in the small VLPs.

Comparison with VP1 of Polymaviruses

The L1 subunit is clearly a close relative of VP1 of polyomaviruses, despite the absence of recognizable sequence similarity. Both form pentamers with radially oriented jelly roll domains; both link to each other through G strand interchange; both use C-terminal projections to form interpentamer contacts and to permit the six distinct packing environments for the subunit in the virion (Liddington et al., 1991). The outer surface loops of L1 are substantially longer than the corresponding loops of VP1—especially FG and HI, the two that make contact across an intervening monomer—but even the frameworks of the jelly roll domains are not readily superimposed. The two sheets formed by CHEF by BIDG of L1

lie more or less parallel to each other, while those of VP1 pack so that the β sandwich opens up toward the five-fold axis. Moreover, when the pentamer axes are aligned, the L1 jelly roll domain tilts away from the axis by 24° relative to VP1, so that the L1 pentamer is substantially wider at its base.

The most striking and unexpected difference between L1 and VP1 is the nature of the C-terminal, interpentamer linkages. The C-terminal arm of polyoma and SV40 VP1 is extended and flexible when the subunit is part of an unassembled pentamer (Stehle and Harrison, 1997; Chen et al., 1998). In the shell of the virion, each arm invades a neighboring pentamer, where it contributes an extra strand (β J) to the B edge of the BIDG sheet of one subunit and forms additional, partly Ca^{2+} -dependent contacts to another (Liddington et al., 1991; Stehle et al., 1994). Moreover, the β J strand is clamped in place by a further strand (β A) from an N-terminal arm of the receiving subunit. Flexibility—the capacity to form a 72-pentamer structure—resides in the freedom of the arm to emerge from the jelly roll core in various directions and in the ability of the proximal residues of the arm to pack against other arms in somewhat variable ways. In the T = 1 particles seen in our crystals, the C-terminal



Figure 4. Amino Acid Sequences of Papillomavirus L1 Proteins

Alignment of L1 sequences from three human papillomavirus types (HPV16, 18, and 11), cottontail rabbit papillomavirus (CRPV), and bovine papillomavirus type 1 (BPV1) (PV website, 1997: <http://hvp-web.lanl.gov>). The secondary structural elements identified from the the HPV16 L1 crystal structure are shown as arrows (strands) and rectangular bars (helices) in the line above the sequences. Blue, pink, and yellow colors have the same significance as in Figure 3A. The numbers refer to the sequence of HPV16.

part (residues 383–474) of the L1 polypeptide chain forms a projecting structure that presents acceptor and donor interaction surfaces, while remaining anchored to the jelly roll domain from which it emanates. Flexibility appears to reside in the extended strands that connect the donor surface (h4) to the rest of the subunit.

Control of L1 Assembly

We can in principle imagine that in the 72-pentamer virion, the C-terminal arms actually interchange, rather than return to their subunit of origin. In small VLPs, the arms of interacting pentamers approach each other near the N termini of the h4 helices (Figure 5B), and relatively minor local rearrangements could be sufficient to create an interchanged structure. The data presented in Table 1 and Figure 1 indicate, however, that even in solution, the recombinant L1 pentamers we express in *E. coli* have anchored C-terminal arms, folded back as in the small VLP. C-terminal deletions that include any residues in helix h5, which anchors the arm, make the L1 extremely protease sensitive, indicating that an ordered h5 is important for stability (Table 1). Moreover, treatment of L1 pentamers with trypsin leads to a cleavage in the C-terminal projection, probably near one end of h4, but the short C-terminal fragment thus produced remains associated with the rest of the pentamer, presumably through tight interactions of h5 (data not shown). Full-length recombinant pentamers assemble

in vitro into virion-like shells (Figure 1, left). The conditions that lead to this assembly, which are the same as those that produce small VLPs from N-terminally truncated L1 (Figure 1, center), are unlikely to promote dissociation of the h5 anchor from its site on the subunit to which it belongs and insertion of the anchor at a related site on another pentamer. Thus, we conclude that assembly of virion-size particles can proceed without arm interchange. It is still possible that in vivo assembly in the presence of appropriate chaperones, which might protect exposed h5, does involve arm interchange. This mode of association would be a form of “domain swap,” now documented to occur in many cases in addition to virus assembly (Schlunegger et al., 1997). This possibility can be tested by comparing properties of 72-pentamer particles assembled in vitro with those derived from expression in eukaryotic cells.

Why does deletion of ten N-terminal residues lead to assembly of a 12-pentamer rather than a 72-pentamer shell? The first ordered residue in our structure, Lys-20, lies near h2 in the C-terminal projection. The N terminus of the protein will thus be adjacent to the h3/h4 interpentamer contact, consistent with its observed effects. The amino-terminal, 20-residue segment is also a good candidate to form a structure that can fill interpentamer gaps in virions and VLPs (Figure 4). Unlike the largely basic, C-terminal disordered segment, the N-terminal region of L1 is relatively well conserved, both in length

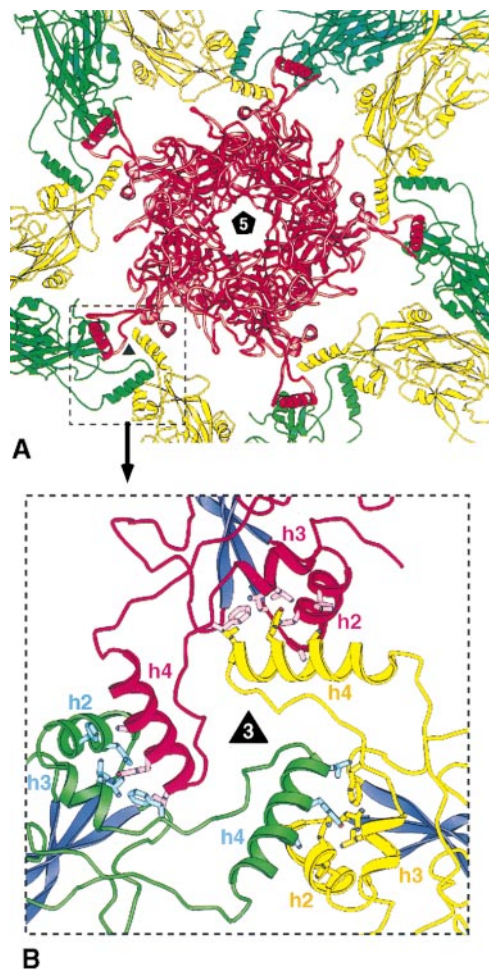


Figure 5. Five-Fold and Three-Fold Interactions in the HPV16 L1 T = 1 Particle

(A) View along a five-fold axis, showing how helix 4 from each subunit projects laterally and rests in a cradle formed by helices 2 and 3 of a subunit in an adjacent pentamer. All subunits in the central pentamer are red; two monomers in each adjacent pentamer are shown in yellow and green, respectively. The region surrounded by a dashed box is magnified in (B), where the contacts around a three-fold axis are displayed in detail. The strands of the β jelly roll in each monomer are blue; the C-terminal projections are red, yellow, and green, corresponding to the colors of the monomers in (A). The hydrophobic side chain contacts between helix 4 and the helix 2-helix 3 cradle are shown explicitly.

and in sequence, and the position of residue 20 is precisely consistent with a gap-filling function. In SV40 and polyoma virions, it is a β hairpin formed by a stretch of about 20 residues at the extreme C terminus of the polypeptide chain that has this role (Liddington et al., 1991).

Two cysteines, conserved among all papillomaviruses, have been reported to participate in VLP formation and virion stabilization, presumably through an interpentamer disulfide bond (Li et al., 1998; Sapp et al., 1998). These residues, 175 and 428 in HPV16, are not linked in our structure, and they are too distant from each other or from any cysteine in a neighboring pentamer to engage in disulfide bonds. In the larger, 72-pentamer shell, helix h4 (the loosely tethered contact

helix: Figure 5B) will have a somewhat different orientation than in the small VLP, and Cys-428 at its C-terminal end may be close enough to Cys-428 of a contacting subunit that the two can form an interpentamer disulfide bridge. A similar set of disulfides appears to occur in SV40, through a cysteine at the base of the CD loop.

L1 Variability

We have used a set of L1 sequences from 49 different HPV types (PV website, 1997: <http://hvp-web.lanl.gov>) to map the correlation of structure and sequence variation. Alignment shows that highly variable stretches are interspersed among segments of conserved residues. Display of conservation in three dimensions by color coding a model (Figure 6) reveals that all the hypervariable regions lie on the outward-facing surface of the pentamer. The lack of conservation may come simply from drift due to weak functional constraints, from negative selection by neutralizing antibodies or other components of an immune response, or from adaptation to the use of different cell surface receptors. Because even the subunits' solvent-exposed lateral faces, which lie beneath the overhang of the star-shaped "cap," are far less variable than the loops on the top, we favor the notion that the changes have been fixed during evolution of the various HPV types by interaction with host functions. There is no evidence for tissue specificity of papillomavirus receptors (Roden et al., 1996a; Evander et al., 1997), and selection for escape from some component of the immune system appears to be the most likely interpretation of the observed pattern of variability.

Potential Receptor Sites

The outer surface of the L1 pentamer has five broad pockets, created by the BC, EF, and FG loops. While the rim of the L1 pocket is extremely variable, the floor is somewhat more conserved. These characteristics make the pockets likely candidates for receptor interaction, and indeed the receptor binding pockets on polyomavirus VP1 are in structurally homologous positions (Stehle et al., 1994; Stehle and Harrison, 1996).

Receptors for papillomaviruses have not been definitively identified. The presence of $\alpha 6$ integrin on the cell surface appears to be required for detectable HPB6b VLP binding, and it has been proposed that members of this class of integrins participate in HPB6b viral uptake (Evander et al., 1997). Functional receptors are present on a broad range of cell types, and bovine and human papillomaviruses can enter by the same pathway (Roden et al., 1996a). Despite their limited host range and tropism, papillomaviruses can bind to cells derived from a variety of tissues and from various species (Roden et al., 1994a; Muller et al., 1995; Volpers et al., 1995). Moreover, particles containing bovine papillomavirus type 1 (BPV1) genomic DNA encapsidated by L1/L2 from either HPV16 or BPV1 can infect the same mouse cell line (Roden et al., 1996a).

Neutralizing Epitopes

Antibody-mediated neutralization of papillomaviruses appears to have at least two distinct mechanisms. Some neutralizing antisera and monoclonal antibodies (mAbs) block cell binding, presumably by steric interference

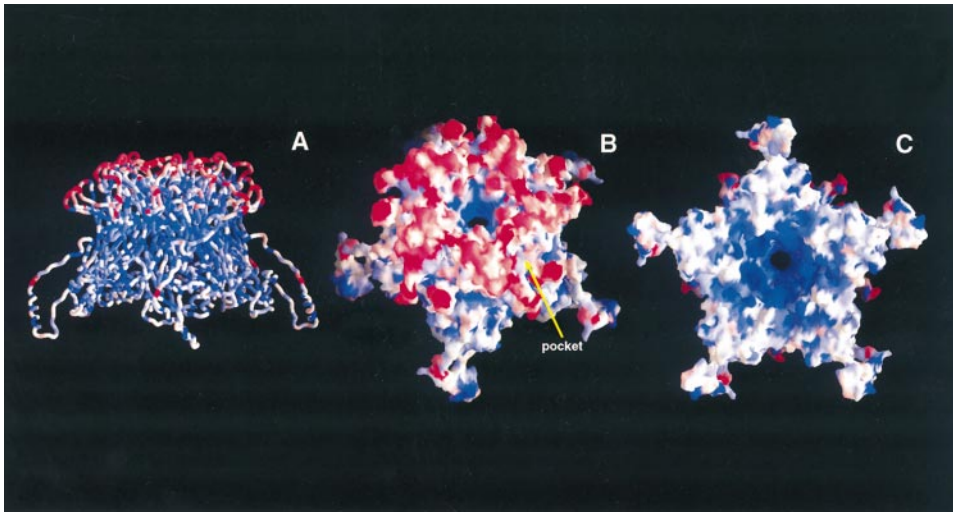


Figure 6. Distribution of L1 Sequence Variation in 49 HPV Types

Highly variable positions are red, fully conserved positions are blue, and positions of intermediate variation are white. (A) Wormlike representation, colored as described, of an L1 pentamer, viewed normal to the five-fold. (B) Surface representation of a tilted "side view" of an L1 pentamer. (C) Interior surface of the pentamer, showing conservation of residues (blue) in the conical cavity along the five-fold axis.

with the receptor site on the virus; others do not prevent attachment (and some even bind cell-attached VLPs) but probably inhibit uncoating (Roden et al., 1994b; Christensen et al., 1995; Booy et al., 1998). Structural analysis by electron cryomicroscopy of BPV1 decorated with two different neutralizing mAbs has yielded images consistent with these alternatives (Trus et al., 1997). One of the mAbs, which blocks attachment, binds to the outer surface of the pentamer; the other, which does not interfere with receptor interaction, binds across the groove between pentamers and presumably stabilizes the particle by cross-linking.

Neutralizing antibodies against papillomaviruses are highly type specific (Roden et al., 1996b). Epitopes have been mapped for neutralizing mAbs raised against HPV16 and HPV11 VLPs (Ludmerer et al., 1996, 1997; Roden et al., 1997; White et al., 1999), and Figure 7A shows positions on the pentamer surface where mutations in L1 influence neutralizing-antibody binding. The site for the V5 epitope of HPV16 lies near the center of the putative receptor pocket, and attachment inhibition is a likely neutralization mechanism. It is possible, however, that an IgG bound at this position could bridge between pentamers in a virion, where the radial divergence of pentamers is less marked than in the small, $T = 1$ particle. The V5 site is a dominant neutralizing epitope on HPV16; the corresponding mAb competes with about 75% of all patient antisera (White et al., 1999).

Within a principal papillomavirus subtype, variants arise with minor differences in L1 sequence; these isolates can differ in their affinity for particular neutralizing mAbs (Roden et al., 1997). The locations of sequence differences in 85 analyzed variants of HPV16 (Figure 7B) are all close to the principal neutralizing epitopes (Figure 7A), consistent with the notion that fixation of these sequence variants is driven by escape from neutralization by antibodies in the host. A distinct pattern of mutations has been observed in 57 variants of HPV5 (Figure

7C), suggesting that there may be a rather different set of dominant neutralization epitopes for different HPV types.

L2 Interactions

Like VP2/3 of the polyomaviruses, L2 probably interacts with an L1 pentamer in the conical hollow that faces inward along the five-fold axis (Griffith et al., 1992). The crystal structure of a complex of a VP1 pentamer and a fragment of VP2/3 shows that the common C-terminal segment of VP2/3 inserts in a looplike fashion into the axial cavity, so that both the N-terminal part of VP2/3 and the very C-terminal part extend toward the interior of the virion (Chen et al., 1998). Side chains that line the corresponding axial cavity in L1 are almost totally conserved, and even the narrow "throat" through which the hollow connects to the exterior contains invariant residues (Figures 6B and 6C). The amino-terminal half of the L2 polypeptide chain is likewise quite conserved. Both extreme amino- and carboxyl termini of L2 are rich in positively charged residues, and it is plausible that both interact with the viral genome. MAb to certain L2 epitopes bind L1/L2 VLPs, however, and some of these mAbs are neutralizing (Campo et al., 1997; Kawana et al., 1999). The neutralizing epitope has in one case been mapped to the vicinity of L2 residue 108 (Kawana et al., 1999). This segment of L2 might project as a loop from the viral shell, either through fenestrations between pentamers or through the throat along the pentamer five-fold axis. Unlike polyomaviruses, where one internal protein associates with each VP1 pentamer, the ratio of L2 chains to L1 pentamers is distinctly substoichiometric. One suggestion is that only the 5-coordinated L1 pentamers contain L2 (Trus et al., 1997), but a more random distribution is also possible.

Vaccine Strategies

VLP-based vaccines are effective in preventing papillomavirus infection in animal models (Breitburd et al.,

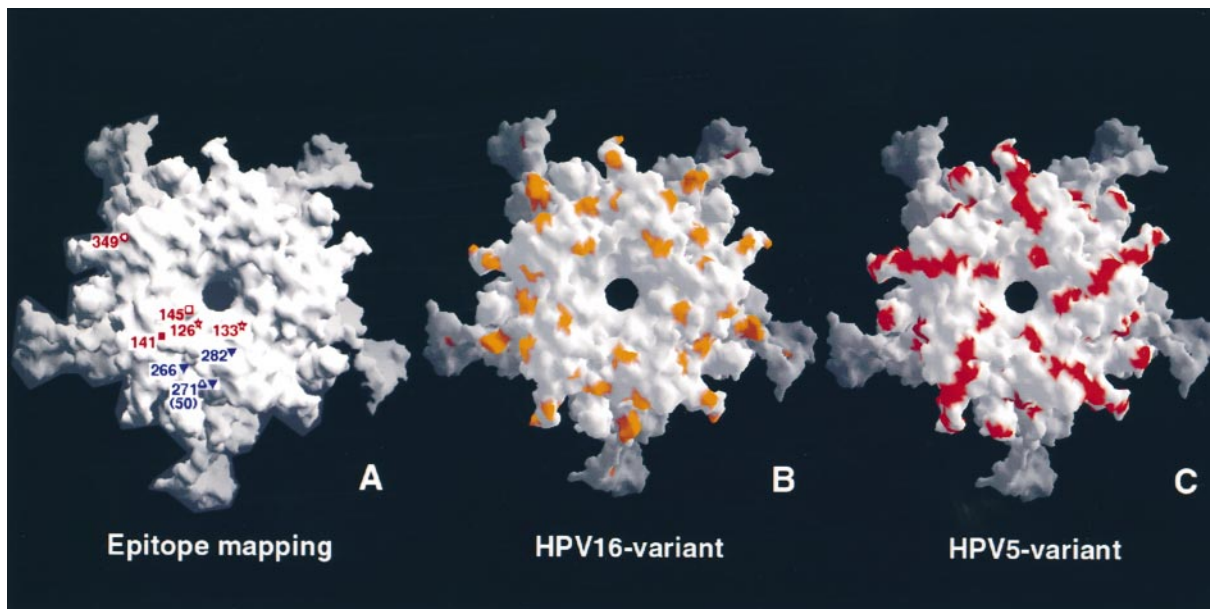


Figure 7. Aspects of the Antigenic Structure of L1

(A) Positions of neutralization epitopes in HPV16 (blue labels) and HPV11 (red labels), shown schematically on a surface representation of the pentamer, viewed along the five-fold axis from the “top.” Only one set of five-fold related sites is shown. Open triangle, H16.V5; closed triangle, H16.E70; star, H11.B2, H11.F1, and H11.G5; closed square, H11.B2 and H11.F1; open square, H11.F1 and H11.G5; open circle, H11.H3. Residue 50, which was shown to affect HPV16 L1 binding to H16.E70 and H16.V5, is situated beneath the surface residue 271 of the FG loop and is likely to influence the loop structure centered on this residue (Ludmerer et al., 1996, 1997; Roden et al., 1997; White et al., 1999). (B) Positions of sequence variation among HPV16 isolates, shown as yellow patches projected onto the outer surface of the L1 pentamer. (C) Positions of sequence variation among HPV5 isolates, shown as red patches on the L1 outer surface.

1995; Suzich et al., 1995; Christensen et al., 1996), and VLP immunogens prepared from yeast and insect cells are now in phase II clinical trials. The L1 structure we

have described has several implications for vaccine design. First, the T = 1 particle itself—in effect, a small VLP—may be a suitable antigen for administration as a

Table 2. Data Collection, Phase Determination, and Refinement Statistics

Data Set	Space Group	a (Å)	Resolution	Completeness	R _{merge}
Native	P2 ₁ 3	387.0	70–3.5 Å (3.62–3.5 Å)	87.5% (56.0%)	12.0% (41.0%)
Mercury	P2 ₁ 3	388.2	70–5.5 Å (5.7–5.5 Å)	88.0% (75.0%)	12.1% (35.6%)
	Phasing from Initial Model Particle		CH ₃ Hg ⁺ SIR Averaging	Phase Extension	
	Before Averaging	After Averaging	Phase Extension		
	70–31 Å	70–31 Å	70–17 Å	25–5.5 Å	25–3.5 Å
Correlation coefficient	37.3%	81%	77%	95.1%	91.2%
R _{avg}	60%	39%	35%	16.9%	25.7%
Refinement R Factors	No Refinement	Final			
		R _{work}	R _{free}		
15–3.5 Å (3.6–3.5 Å)	42%	28.3% (35.2%)	29.1% (36.5%)		

$R_{\text{merge}} = \sum |I - \langle I \rangle| / \sum I$, where I is the observed intensity, and $\langle I \rangle$ is the weighted average intensity of multiple observations of symmetry-related reflections. The sums are over all independent reflections for which there are multiple observations.

$R_{\text{avg}} = \sqrt{\sum [w(F_o - F_c)]^2 / \sum w F_o^2}$, where F_c and F_o are calculated and observed structure factors, and w is a weight for each reflection over which the sum is taken.

$R_{\text{work}} (R_{\text{free}}) = \sum |F_o - F_c| / \sum |F_o|$, where F_c and F_o are the calculated and observed structure factors, and the sums are over all reflections.

Correlation coefficient = $\sum_n (|F_o| - \langle F_o \rangle) (|F_c| - \langle F_c \rangle) / [\sum_n (|F_o| - \langle F_o \rangle)^2 \sum_n (|F_c| - \langle F_c \rangle)^2]^{1/2}$, where F_o and F_c are observed and calculated structure factors, and the sums are over all reflections.

Numbers in parentheses refer to the outermost resolution bin.

vaccine. Presentation of epitopes on individual pentamers is likely to be identical in the two contexts. The higher curvature of a small VLP implies that the pentamer tips are somewhat more widely separated than in a 72-pentamer shell, but the distances suggest that IgGs could still form bridges, if such interactions were important for B cell receptor affinity. The convenience of bacterial expression is significant. Second, the analysis of epitopes and variants in Figure 7 provides a rational approach to cross-protective VLP (or $T = 1$) vaccines, by grafting segments of other HPV types—or even of other proteins—onto the same L1 matrix (Chackerian et al., 1999). Previous efforts to do so have involved effectively random trial and error. Third, the structure suggests how new interpentamer interactions could be introduced to stabilize the $T = 1$ particles, and through model-building, the 72-pentamer VLPs as well. Efforts to obtain the structure of a 72-pentamer particle, by fitting the results of high-resolution electron cryomicroscopy (Trus et al., 1997) and perhaps by crystallizing VLPs, are clearly relevant in this regard. Finally, by analogy with our previous work on polyomavirus VP1/VP2 complexes (Chen et al., 1998), we can now devise strategies for determining the location of L2 neutralizing epitopes, through studies of appropriate coassemblies.

Experimental Procedures

Protein Preparation and Crystallization

Recombinant HPV16 L1 was expressed in *E. coli* as a GST fusion protein, using the pGEX-2T expression vector, and purified from the supernatant of disrupted cells by glutathione-Sepharose chromatography. As described in greater detail elsewhere (X. S. C. et al., unpublished data), it was necessary to add ATP and 3.5 M urea to the cell lysate to release tightly bound GroEL. The GST moiety was removed by thrombin cleavage; subsequent Superdex chromatography yielded pure L1 pentamers. During crystallization trials, only the deletion mutant lacking the N-terminal ten amino acids yielded good crystals in the presence of 7.5% PEG in 0.2 M NaOAc buffer (pH 4.5). We obtained several crystal forms; the space group of the form used to determine the structure was P2₁3, $a = 387 \text{ \AA}$.

In Vitro Assembly

Purified pentamers produced by the corresponding deletion constructs (Table 1) were diluted from 10 mg/ml to 10 μ g/ml with buffer containing 0.2 M Na acetate (pH 5.2), 1 M NaCl and allowed to stand at room temperature for 30 min. Samples were then spotted onto glow-discharged, carbon-coated grids and stained with 2% uranyl acetate for electron microscopy with a JEOL 100-CX microscope, operated at 80 kV.

Data Collection

Both native and mercury derivative (methyl mercury hydroxide) data sets were recorded at the CHESS F1 beamline with the ACSD Quantum-4 ccd detector. Native data extended to 3.5 \AA ; derivative data, to 5.5 \AA . The data were indexed and integrated with DENZO (Otwinowski and Minor, 1997) and further processed with SCALEPACK and CCP4 programs (Collaborative Computational Project, 1994; version ccp4_3.3). Statistics are in Table 2. The mean $I/\sigma(I)$ in the last resolution bin is about 2.

Phase Determination

Initial, very low resolution phases were obtained by molecular replacement with an approximate model, in which the polyomavirus VP1 pentamer was used as a five-fold symmetric "lump" of about the correct size. Self-rotation functions were used to determine the particle orientation (a single parameter in this space group), and a single-parameter position search along the crystallographic three-fold was used to find the particle center. Two internal parameters

of the particle (pentamer azimuth and radius) were refined against the observed data, using structure-factor correlation as a target, before the initial phase calculation. Phases at very low resolution (70–31 \AA) were refined and extended to 17 \AA by 20-fold noncrystallographic symmetry (NCS) averaging using RAVE (Kleywegt and Jones, 1994). This phase set was adequate for locating the 120 mercury sites in a crystallographic asymmetric unit. Further 20-fold NCS averaging and phase extension based on the mercury SIR phases yielded a 3.5 \AA resolution map with clear side chain features, into which the L1 model was built using the program O (Jones et al., 1991). Details of the structure determination will be published elsewhere (Chen and Harrison, unpublished data).

Refinement

The initial model had an R factor of 42% (8–3.5 \AA). Using 20-fold NCS restraints throughout the calculations, 300 steps of positional refinement in CNS (Brünger et al., 1998) gave $R_{\text{work}} = 34.5\%$ and $R_{\text{free}} = 35.8\%$. Torsion-angle molecular dynamics refinement lowered these figures to 33.4% and 34.9%, respectively. Further thermal-parameter (B) refinement together with positional refinement using data between 15 and 3.5 \AA yielded $R_{\text{work}} = 28.3\%$ and $R_{\text{free}} = 29.1\%$ (see Table 2). All residues of the final model have ϕ/ψ angles in the allowed regions of a Ramachandran plot (PROCHECK: Laskowski et al., 1993), with 72% in the most favored region.

Illustrations

The figures were made using O (Jones et al., 1991) (Figure 2), Molscript (Kraulis, 1991) (Figure 3), Ribbons (Carson, 1987) (Figure 5), and GRASP (Nicholls et al., 1991) (Figures 6 and 7).

Acknowledgments

We thank Dan Thiel and the staff at CHESS and MacCHESS for assistance with data collection, colleagues in Harrison/Wiley laboratory for helpful discussion, Thilo Stehle (MGH) for advice, Liang Tong (Columbia University) for providing us with his GLRF programs for the self-rotation function, Maolin Li for preparation of HPV11 L1, and Barbara Harris for assistance with crystal growth. The work was supported by NIH grants CA-13202 (to S. C. H.) and CA-37667 (to R. L. G.). S. C. H. is an investigator in the Howard Hughes Medical Institute.

Received November 16, 1999; revised December 28, 1999.

References

- Baker, T.S., Newcomb, W.W., Olson, N.H., Cowser, L.M., Olson, C., and Brown, J.C. (1991). Structures of bovine and human papillomaviruses. Analysis by cryoelectron microscopy and three-dimensional image reconstruction. *Biophys. J.* 60, 1445–1456.
- Belnap, D.M., Olson, N.H., Cladel, N.M., Newcomb, W.W., Brown, J.C., Kreider, J.W., Christensen, N.D., and Baker, T.S. (1996). Conserved features in papillomavirus and polyomavirus capsids. *J. Mol. Biol.* 259, 249–263.
- Booy, F.P., Roden, R.B., Greenstone, H.L., Schiller, J.T., and Trus, B.L. (1998). Two antibodies that neutralize papillomavirus by different mechanisms show distinct binding patterns at 13 \AA resolution. *J. Mol. Biol.* 281, 95–106.
- Bosch, F.X., Manos, M.M., Munoz, N., Sherman, M., Jansen, A.M., Peto, J., Schiffman, M.H., Moreno, V., Kurman, R., and Shah, K.V. (1995). Prevalence of human papillomavirus in cervical cancer: a worldwide perspective. International biological study on cervical cancer (IBSCC) Study Group. *J. Natl. Cancer Inst.* 87, 796–802.
- Breitbart, F., Kirnbauer, R., Hubbert, N.L., Nonnenmacher, B., Trindinh-Desmarquet, C., Orth, G., Schiller, J.T., and Lowy, D.R. (1995). Immunization with viruslike particles from cottontail rabbit papillomavirus (CRPV) can protect against experimental CRPV infection. *J. Virol.* 69, 3959–3963.
- Brünger, A.T., Adams, P.D., Clore, G.M., Delano, W.L., Gros, P., Grosse-Kunstleve, R.W., Jiang, J.-S., Kuszewski, J., Nilges, M., Pannu, N.S., et al. (1998). Crystallography and NMR system: a new

- software suite for macromolecular structure determination. *Acta Crystallogr. D* 54, 901–921.
- Campo, M.S., O'Neil, B.W., Grindlay, G.J., Curtis, F., Knowles, G., and Chandrachud, L. (1997). A peptide encoding a B-cell epitope from the N-terminus of the capsid protein L2 of bovine papillomavirus-4 prevents disease. *Virology* 234, 261–266.
- Carson, M. (1987). Ribbon models of macromolecules. *J. Mol. Graph.* 5, 103–106.
- Chackerian, B., Lowy, D.R., and Schiller, J.T. (1999). Induction of autoantibodies to mouse CCR5 with recombinant papillomavirus particles. *Proc. Natl. Acad. Sci. USA* 96, 2373–2378.
- Chen, X.S., Stehle, T., and Harrison, S.C. (1998). Interaction of polyomavirus internal protein VP2 with the major capsid protein VP1 and implications for participation of VP2 in viral entry. *EMBO J.* 17, 3233–3240.
- Christensen, N.D., Cladel, N.M., and Reed, C.A. (1995). Postattachment neutralization of papillomaviruses by monoclonal and polyclonal antibodies. *Virology* 207, 136–142.
- Christensen, N.D., Reed, C.A., Cladel, N.M., Han, R., and Kreider, J.W. (1996). Immunization with viruslike particles induces long-term protection of rabbits against challenge with cottontail rabbit papillomavirus. *J. Virol.* 70, 960–965.
- Collaborative Computational Project, Number 4 (1994). The CCP4 suite: programs for crystallography. *Acta Crystallogr. D* 50, 760–763.
- Evander, M., Frazer, I.H., Payne, E., Qi, Y.M., Hengst, K., and McMillan, N.A. (1997). Identification of the alpha6 integrin as a candidate receptor for papillomaviruses. *J. Virol.* 71, 2449–2456.
- Greenstone, H.L., Nieland, J.D., deVisser, K.E., De Bruijn, M.L., Kirnbauer, R., Roden, R.B., Lowy, D.R., Kast, W.M., and Schiller, J.T. (1998). Chimeric papillomavirus-like particles elicit antitumor immunity against the E7 oncoprotein in an HPV16 tumor model. *Proc. Natl. Acad. Sci. USA* 95, 1800–1805.
- Griffith, J.P., Griffith, D.L., Rayment, I., Murakami, T., and Caspar, D.L.D. (1992). Inside polyomavirus at 25-Å resolution. *Nature* 355, 652–654.
- Hagensee, M.E., Yaegashi, N., and Galloway, D.A. (1993). Self-assembly of human papillomavirus type 1 capsids by expression of the L1 protein alone or by coexpression of the L1 and L2 capsid proteins. *J. Virol.* 67, 315–322.
- Howley, P. (1996). *Papillomavirinae: the Viruses and Their Replication* (New York: Raven Press).
- Jones, T.A., Zhou, J.-Y., Cowan, S.W., and Kjeldgaard, M. (1991). Improved methods for building protein models in electron density maps and the location of errors in these models. *Acta Crystallogr. A* 47, 110–119.
- Kawana, K., Yoshikawa, H., Taketani, Y., Yoshiike, K., and Kanda, T. (1999). Common neutralization epitope in minor capsid protein L2 of human papillomavirus types 16 and 6. *J. Virol.* 73, 6188–6190.
- Kirnbauer, R., Booy, F., Cheng, N., Lowy, D.R., and Schiller, J.T. (1992). Papillomavirus L1 major capsid protein self-assembles into virus-like particles that are highly immunogenic. *Proc. Natl. Acad. Sci. USA* 89, 12180–12184.
- Kirnbauer, R., Taub, J., Greenstone, H., Roden, R., Durst, M., Gissmann, L., Lowy, D.R., and Schiller, J.T. (1993). Efficient self-assembly of human papillomavirus type 16 L1 and L1-L2 into virus-like particles. *J. Virol.* 67, 6929–6936.
- Kleywegt, G.J., and Jones, T.A. (1994). From first map to final model. In *Proceedings of the CCP4 Study Weekend*, S. Bailey, R. Hubbard, and D. Waller, eds. (Daresbury, UK: Daresbury Laboratory), pp. 59–66.
- Kraulis, P.E. (1991). MOLSCRIPT: a program to produce both detailed and schematic plots of protein structures. *J. Appl. Crystallogr.* 24, 946–950.
- Laskowski, R.A., MacArthur, M.W., Moss, D.S., and Thornton, J.M. (1993). PROCHECK—a program to check the stereochemical quality of protein structures. *J. Appl. Crystallogr.* 26, 283–291.
- Li, M., Beard, P., Estes, P.A., Lyon, M.K., and Garcea, R.L. (1998). Intercapsomeric disulfide bonds in papillomavirus assembly and disassembly. *J. Virol.* 72, 2160–2167.
- Liddington, R.C., Yan, Y., Zhao, H.C., Sahli, R., Benjamin, T.L., and Harrison, S.C. (1991). Structure of simian virus 40 at 3.8 Å resolution. *Nature* 354, 278–284.
- Ludmerer, S.W., Benincasa, D., and Mark, G.E., III. (1996). Two amino acid residues confer type specificity to a neutralizing, conformationally dependent epitope on human papillomavirus type 11. *J. Virol.* 70, 4791–4794.
- Ludmerer, S.W., Benincasa, D., Mark, G.E., III, and Christensen, N.D. (1997). A neutralizing epitope of human papillomavirus type 11 is principally described by a continuous set of residues which overlap a distinct linear, surface-exposed epitope. *J. Virol.* 71, 3834–3839.
- Muller, M., Gissmann, L., Cristiano, R.J., Sun, X.Y., Frazer, I.H., Jenson, A.B., Alonso, A., Zentgraf, H., and Zhou, J. (1995). Papillomavirus capsid binding and uptake by cells from different tissues and species. *J. Virol.* 69, 948–954.
- Muller, M., Zhou, J., Reed, T.D., Rittmuller, C., Burger, A., Gabelsberger, J., Braspenning, J., and Gissmann, L. (1997). Chimeric papillomavirus-like particles. *Virology* 234, 93–111.
- Nicholls, A., Sharp, K.A., and Honig, B. (1991). Protein folding and association: insights from the interfacial and thermodynamic properties of hydrocarbons. *Proteins* 11, 281–296.
- Otwinowski, Z., and Minor, W. (1997). Processing of x-ray diffraction data collected in oscillation mode. *Methods Enzymol.* 276, 307–326.
- Pisani, P., Parkin, D.M., and Ferlay, J. (1993). Estimates of the worldwide mortality from eighteen major cancers in 1985. Implications for prevention and projections of future burden. *Int. J. Cancer* 55, 891–903.
- Rayment, I., Baker, T.S., Caspar, D.L.D., and Murakami, W.T. (1982). Polyoma virus capsid structure at 22.5 Å resolution. *Nature* 295, 110–115.
- Roden, R.B., Kirnbauer, R., Jenson, A.B., Lowy, D.R., and Schiller, J.T. (1994a). Interaction of papillomaviruses with the cell surface. *J. Virol.* 68, 7260–7266.
- Roden, R.B., Weissinger, E.M., Henderson, D.W., Booy, F., Kirnbauer, R., Mushinski, J.F., Lowy, D.R., and Schiller, J.T. (1994b). Neutralization of bovine papillomavirus by antibodies to L1 and L2 capsid proteins. *J. Virol.* 68, 7570–7574.
- Roden, R.B., Greenstone, H.L., Kirnbauer, R., Booy, F.P., Jessie, J., Lowy, D.R., and Schiller, J.T. (1996a). In vitro generation and type-specific neutralization of a human papillomavirus type 16 virion pseudotype. *J. Virol.* 70, 5875–5883.
- Roden, R.B., Hubbert, N.L., Kirnbauer, R., Christensen, N.D., Lowy, D.R., and Schiller, J.T. (1996b). Assessment of the serological relatedness of genital human papillomaviruses by hemagglutination inhibition. *J. Virol.* 70, 3298–3301.
- Roden, R.B., Armstrong, A., Haderer, P., Christensen, N.D., Hubbert, N.L., Lowy, D.R., Schiller, J.T., and Kirnbauer, R. (1997). Characterization of a human papillomavirus type 16 variant-dependent neutralizing epitope. *J. Virol.* 71, 6247–6252.
- Rose, R.C., Bonnez, W., Reichman, R.C., and Garcea, R.L. (1993). Expression of human papillomavirus type 11 L1 protein in insect cells: in vivo and in vitro assembly of viruslike particles. *J. Virol.* 67, 1936–1944.
- Sapp, M., Fligge, C., Petzak, I., Harris, J.R., and Streeck, R.E. (1998). Papillomavirus assembly requires trimerization of the major capsid protein by disulfides between two highly conserved cysteines. *J. Virol.* 72, 6186–6189.
- Sasagawa, T., Pushko, P., Steers, G., Gschmeissner, S.E., Hajibagheri, M.A., Finch, J., Crawford, L., and Tommasino, M. (1995). Synthesis and assembly of virus-like particles of human papillomaviruses type 6 and type 16 in fission yeast *Schizosaccharomyces pombe*. *Virology* 206, 126–135.
- Schlunegger, M.P., Bennett, M.J., and Eisenberg, D. (1997). Oligomer formation by 3D domain swapping: a model for protein assembly and misassembly. *Adv. Prot. Chem.* 50, 61–122.
- Shah, K.V., and Howley, P. (1996). *Papillomaviruses* (New York: Raven Press).
- Stehle, T., Yan, Y., Benjamin, T.L., and Harrison, S.C. (1994). Structure of murine polyomavirus complexed with an oligosaccharide receptor fragment. *Nature* 369, 160–163.
- Stehle, T., and Harrison, S.C. (1996). Crystal structures of murine

polyomavirus in complex with straight-chain and branched-chain sialyloligosaccharide receptor fragments. *Structure* 4, 183–194.

Stehle, T., and Harrison, S.C. (1997). High-resolution structure of a polyomavirus VP1-oligosaccharide complex: implications for assembly and receptor binding. *EMBO J.* 16, 5139–5148.

Suzich, J.A., Ghim, S.J., Palmer-Hill, F.J., White, W.I., Tamura, J.K., Bell, J.A., Newsome, J.A., Jenson, A.B., and Schlegel, R. (1995). Systemic immunization with papillomavirus L1 protein completely prevents the development of viral mucosal papillomas. *Proc. Natl. Acad. Sci. USA* 92, 11553–11557.

Trus, B.L., Roden, R.B., Greenstone, H.L., Vrhel, M., Schiller, J.T., and Booy, F.P. (1997). Novel structural features of bovine papillomavirus capsid revealed by a three-dimensional reconstruction to 9 Å resolution. *Nat. Struct. Biol.* 4, 413–420.

Volpers, C., Unckell, F., Schirmacher, P., Streeck, R.E., and Sapp, M. (1995). Binding and internalization of human papillomavirus type 33 virus-like particles by eukaryotic cells. *J. Virol.* 69, 3258–3264.

White, W.I., Wilson, S.D., Palmer-Hill, F.J., Woods, R.M., Ghim, S.J., Hewitt, L.A., Goldman, D.M., Burke, S.J., Jenson, A.B., Koenig, S., and Suzich, J.A. (1999). Characterization of a major neutralizing epitope on human papillomavirus type 16 L1. *J. Virol.* 73, 4882–4889.

Zhou, J., Sun, X.Y., Stenzel, D.J., and Frazer, I.H. (1991a). Expression of vaccinia recombinant HPV 16 L1 and L2 ORF proteins in epithelial cells is sufficient for assembly of HPV virion-like particles. *Virology* 185, 251–257.

Zhou, J., Doorbar, J., Sun, X.Y., Crawford, L.V., McLean, C.S., and Frazer, I.H. (1991b). Identification of the nuclear localization signal of human papillomavirus type 16 L1 protein. *Virology* 185, 625–632.

Protein Data Bank ID Code

The ID code for the coordinates of the structure reported in this article is 1dzl.